Electrophysiological and behavioral phenotype of insulin receptor defective mice

P. Das[a], **A.D. Parsons**[b], **J. Scarborough**[a], **J. Hoffman**[a], **J. Wilson**[a], **R.N. Thompson**[a], **J.M. Overton**[b], and **D.A. Fadool**[a,*]

[a]Department of Biological Science, Programs in Neuroscience and Molecular Biophysics, 214 Biomedical Research Facility, Florida State University, Tallahassee, FL 32306, USA

[b]Department of Nutrition, Food and Exercise Science, Program in Neuroscience, The Florida State University, Tallahassee, FL 32306, USA

Abstract

The olfactory bulb expresses one of the highest levels of insulin found in the brain. A high level of expression of the concomitant insulin receptor (IR) kinase is also retained in this brain region, even in the adult. We have previously demonstrated in a heterologous system that insulin modulates the voltage-dependent potassium channel, Kv1.3, through tyrosine phosphorylation of three key residues in the amino and carboxyl terminus of the channel protein. Phosphorylation also induces current suppression of the Kv1.3-contributed current in cultured olfactory bulb neurons (OBNs) of rodents. In order to explore the behavioral importance of this kinase-induced modulation of the channel for the olfactory ability of the animal, mice with a targeted-gene deletion of the insulin receptor were electrophysiologically and behaviorally characterized. Mice heterozygous for the insulin receptor kinase (IR+/−) gene performed the same as wild-type (+/+) mice when challenged with a traditional, non-learning-based task to test gross anosmia. There was also no significant difference across the two genotypes in tests designed to measure exploratory behavior or in a battery of systems physiology experiments designed to assess metabolic energy usage (locomotion, ingestive behaviors, weight, oxygen consumption, and respiratory quotient). Object memory recognition tests suggest that IR+/− mice have an impairment in recognition of familiarized objects; IR+/− mice demonstrate poor performance for both short-term (1 h) and long-term (24 h) memory tests in comparison to that of wild-type mice. Electrophysiological experiments indicate that mitral cell neurons cultured from both heterozygous and homozygous-null mice (IR+/− and IR−/−) have an decreased peak current amplitude compared with that recorded for wild-type (+/+) animals matched for days in vitro (DIV). These data indicate that the loss of one allele of the IR kinase gene modifies the electrical phenotype of the mitral cell neurons in the olfactory bulb without a change in gross olfactory ability. Given our findings that there are no significant changes in metabolic balance of the IR (+/−) mice but some impairment in memory retention, future experiments testing for specific olfactory behaviors or functional deficits in IR−/+ mice models of diabetes will need to either be tasks that do not require learning or will require a different model (such as diet-induced diabetes) that may evoke a stronger phenotype.

Keywords

Olfactory; IR kinase; Potassium channel; Kv1.3; Diabetes; Memory

*Corresponding author. Tel.: +1 850 644 4775; fax: +1 850 645 3281. *E-mail address*:dfadool@bio.fsu.edu (D.A. Fadool).

1. Introduction

Given the wealth of accumulated knowledge with regards to peripheral insulin signaling, our understanding of the role of brain insulin is comparatively sparse [19]. The hormone insulin is abundantly present in the central nervous system (CNS), where it is thought to be transported, rather than cerebrally synthesized, across the blood–brain barrier as a regulatory peptide [3]. IR kinases are richly expressed in different brain regions including the olfactory bulb, cerebral cortex, hippocampus, amygdaloid nucleus, hypothalamus, septum, the substantia nigra, basal ganglia and the frontal cortex [5,13,51]. The olfactory bulb, in particular, is reported to contain 56 ng/g insulin [20]. This is a concentration representing the highest of all brain regions [5] and yet few studies have explored phosphorylation by insulin signaling in the olfactory system [4,11,15,30].

Not including olfactory centers (olfactory bulb and cortex), recent evidence indicates that brain insulin and IR kinase play key roles in learning and memory formation, synaptic plasticity, and axonal guidance [14,38,44]. Acute intracerebro-ventricular administration of insulin has been shown to enhance memory in a passive avoidance behavioral paradigm suggesting that hyperinsulinemia may modulate cognition [34]. Rats treated with streptozocin, a drug that diminishes production and secretion of insulin through permanent destruction of the Islets of Langerhans, also produces severe impairment in learning and memory as determined by the Morris water maze task [6,7,27]. While disruption or enhancement of insulin action causes changes in learning and memory, learning itself can also cause upregulation of molecules associated with insulin signaling. For example, IR kinase was significantly increased in the hippocampus of rats trained in a spatial maze learning task [50]. Taken together, these studies suggest that insulin and IR kinase may be involved in normal memory function [13]. In addition, brain insulin signaling regulates behavior and systems physiology; including energy homeostasis, body weight, food intake and fuel metabolism. Brain/ neuron-specific disruption of the IR gene in mice has been shown to increase dietary intake and thus obesity [9].

The molecular basis of diverse actions of insulin in the brain may be the activation of several downstream signaling molecules. Activation of IR kinase causes multiple tyrosine phosphorylation of the insulin receptor substrate (IRS), a downstream effector in the signaling cascade [2,39]. In brain regions such as the olfactory bulb, however, IRS is weak or absent [18]. Data from our laboratory support the idea that in the absence of the traditional IRS, an ion channel protein, Kv1.3, may serve as a downstream substrate for IR kinase in the olfactory bulb [17]. Kv1.3 is a delayed rectifier and member of the *Shaker* family of voltage-gated potassium channels [10,23,33,40]. Kv1.3 has been shown through pharmacological block to carry 60–80% of the outward current in mitral cells of the olfactory bulb [11,15]. Activation of IR kinase in these neurons causes Kv1.3 current suppression but no change in channel kinetics as measured via whole-cell electrophysiology experiments where insulin is acutely applied to the recording bath [15]. It is also likely that IR kinase selectively modulates Kv1.3 as opposed to other Kv family members expressed in the mitral cell neurons (Kv1.4 and Kv1.5) because in analogous electrophysiological experiments using Kv1.3-null mice, whole-cell current is not modulated by insulin [16]. Like IRS, Kv1.3 becomes multiply tyrosine phosphorylated by activated IR kinase (channel residues Y111, Y112, Y113, Y137, and Y449) in the cytoplasmic aspect of the channel, which could then serve as recognition motifs for protein–protein interactions with neighboring SH2 domain containing proteins [17]. Similar to the transitory relationship between IR kinase and IRS in the periphery, co-immunoprecipitation experiments fail to demonstrate a direct association of the Kv1.3 channel with IR kinase (Fadool, unpublished data), potentially reflecting the requirement of intermediate adaptor proteins.

Regardless of whether there is a tight association, modulation of the Kv1.3 channel by IR kinase is complex, affected by sensory experience, dietary restriction, and the channel itself is shown to reciprocally down-regulate the IR kinase activity of the enzyme [17]. For example, OBNs harvested from animals that are odor-sensory deprived from birth via unilateral naris-occlusion fail to be modulated by insulin [17]. Unlike peripheral insulin, fasting induces an elevation of insulin in the OB [17], presumably decreasing the activity of Kv1.3 to increase the sense of smell [16]. Finally, as revealed in heterologous expression systems, the expression of the channel decreases the phosphorylation of the IR kinase, although the kinase initially acts to suppress channel current [11,15]. This level of combined complexity in the signalling relationship between the Kv1.3 channels and the IR kinase in a brain region known to express large quantities of the hormone insulin, led us to probe the olfactory behavior and biophysical properties of OBN in mice with targeted deletion of the IR kinase gene.

2. Methods

2.1. Solutions and antisera

Olfactory bulb neuron (OBN) patch pipette solution contained (in mM): 145 KCl, 10 HEPES, 10 EGTA, 2 $MgCl_2$, 0.20 NaATP, 0.5 GTP (pH 7.3). OBN bath recording solution contained (in mM): 150 NaCl, 5 KCl, 2.6 $CaCl_2$, 2 $MgCl_2$, and 10 HEPES (pH 7.3). Patch pipette and bath recording solutions were formulated to maximize Kv1.3 currents. Homogenization buffer (HB) contained (in mM): 320 sucrose, 10 Tris base, 50 KCl, 1 EDTA (pH 7.8); with the addition of phosphatase and protease inhibitors (PPI): 1 sodium orthovanadate, 1 phenylmethylsulfonyl fluoride (PMSF), 10 µg/ml aprotinin, 1 µg/ml leupeptin, and 1 µg/ml pepstatin A. Phosphate-buffered saline (PBS) contained (in mM): 136.9 NaCl, 2.7 KCl, 10.1 Na_2HPO_4, 1.8 KH_2PO_4 (pH 7.4). 0.01M Tris buffer (500 ml) contained: 3.3 ml 1.5 M Tris pH 8.8, 50 ml 10% SDS, 357 µl β-mercaptoethanol, to volume with water. 3 M sodium citrate buffer (pH 3.0; 500 ml) contained: 14.70 g sodium citrate, 50 ml 10% SDS, 357 µl β-mercaptoethanol, to volume with water. Tissue culture reagents were purchased from Gibco/BRL (Gaithersburg, MD). DMEM contained Dulbecco's minimal essential medium supplemented with 5% fetal bovine serum and 2% penicillin–streptomycin sulfate. All salts were purchased from Sigma Chemical Co. (St. Louis, MO) or Fisher Scientific (Houston, TX).

α-Kv1.3 antibody (AU13), a rabbit polyclonal antiserum, was generated against the 46 amino acid sequence 478 MVIEEGGMNHSAFPQTPFKTGNSTATCTTNNNPNDCV NIKKIFTDV 523 representing the unique coding region of Kv1.3 between the carboxyl terminus and transmembrane domain 1. The purified peptide was produced by Genmed Synthesis (San Francisco, CA) and the antisera was produced by Cocalico Biologicals (Reamstown, PA). This antibody has been previously characterized [41] and was currently used for Western blot detection (1 : 1500) of Kv1.3 in the olfactory bulb of wild-type (wt) (+/+) and heterozygous-null IR (+/−) mice. Monoclonal antiserum directed against amino acids 156–322 of human TrkB was purchased from Transduction Laboratories (San Diego, CA) and used at 1:800 for Western blots.

2.2. Mouse breeding and genotyping

Heterozygous B6.129S4-*Insr^tm1 Dac*/J mice (donor strain = 129S4 via J1 ES cell line using C57BL/6 background strain) containing a null allele of the insulin receptor gene were purchased from Jax Laboratories (stock # 002939; Jacksonville, FL) [1]. Control wild-type (wt) animals were similarly purchased as C57BL/6J (stock # 000664). Mice were maintained in the laboratory animal care facility at Florida State University and genotyped by standard tail biopsy [22] using DNAeasy tissue extraction kit (Qiagen, Valencia, CA) for tail DNA isolation. The premature chain termination mutation was designed based upon similar mutations identified in insulin-resistant patients and was introduced downstream from codon 306 in exon

4 to disrupt proper translation of the IR kinase gene [1]. Because homozygous-null (IR−/−) mice undergo diabetic ketosis within 24–72 h of birth, matings between heterozygous-null (IR +/−) mice were used to produce homozygous-null (IR−/−) animals with expected Mendelian frequency. In order to standardize collection of OB neurons at the same stage of IR development, animals were harvested as appropriate for physiology, behavior, or biochemistry. For primary cell culture, all three expected progeny (IR−/−, IR+/−, and wt+/+) were sacrificed blind at postnatal day (P) 1 (24 h after birth) to obtain neurons for electrophysiological studies with genotyping performed following the recordings. At this stage (P1), all animals appear healthy (indistinguishable) so the entire litter is harvested and then electrophysiological recordings are sorted post hoc when the genotyping is completed. Since our previous work in rat has demonstrated a plateau of IR kinase expression at P20 in the olfactory bulb [17], this postnatal stage was selected for protein biochemistry of generated IR (+/−) mice. Mature IR (+/−) mice (P60 or greater) were used for behavioral and metabolic experiments. The genotyping PCR protocol was as defined by Jax laboratories for this gene-targeted deletion with modification to include a hot start and touchdown annealing design. The following primers were used to detect the wild-type (wt) and mutant (mt) allele, respectively: forward wt=5′ctt gat gtg cac ccc atg tct 3′ reverse wt=5′tcg gat gtt gat gat cag gct 3′; forward mt = 5′gat cgg cca ttg aac aag atg 3′; reverse mt = 5′cgc caa gct ctt cag caa tat 3′.

2.3. Protein biochemistry

Postnatal day twenty (P20) mice (IR+/− and wt+/+) were euthanized with CO2 inhalation and rapid decapitation as per Florida State University Laboratory Animal Resources and AVMA-approved methods. The olfactory bulbs (OBs) were quickly harvested and homogenized in HB +PPI (see Solutions) for fifty strokes with a Kontes (#20) tissue grinder on ice (Vineland, NJ). Membrane proteins were isolated as previously described [41]. Thirty micrograms of purified membrane proteins were separated on 10% acrylamide gels by SDS-PAGE and electro-transferred to nitrocellulose blots [37]. Blots were blocked with 4% non-fat milk (Bio-rad, Hercules, CA) and incubated overnight at 4 °C with primary antibodies against Kv1.3 or TrkB (see Solutions and antisera). Species-specific horseradish peroxidase-conjugated secondary antibodies were applied at room temperature for 90 min. Labeled proteins were visualized by exposure of Fugi Rx film (Fisher) to enhanced chemiluminescence (ECL, Amersham-Pharmacia, Piscataway NJ). Obtained autoradiographs were analyzed by quantitative densitometry using a Hewlett-Packard PhotoSmart Scanner (model 106–816, Hewlett-Packard, San Diego, CA) in conjunction with Quantiscan software (Biosoft, Cambridge, England) using a line scanning method of analysis as previously described [12]. Membrane proteins from wt (+/+) and heterozygous-null IR(+/−) animals were always probed with the same antisera contained on the same piece of nitrocellulose and exposed on the same piece of X-ray film to eliminate difference in ECL exposure. Likewise, blots were stripped with six washes of 0.1M Tris buffer (pH 8.8) and sodium citrate buffer (pH 3.0), respectively, and then re-probed with an antibody directed against β-actin (Sigma Chemical, St. Louis, MO; catalog #A2066, polyclonal antisera) to ensure equal protein loading.

2.4. Primary cell culture

Olfactory bulb neuron cultures were prepared from postnatal day 1 (P1) mice generated from heterozygous crossings (IR+/− ×IR+/−) as previously described for wt mice with minor adjustments [11]. Briefly, mice were rapidly decapitated, pairs of OBs were harvested, and the tissue from individual animals was separately incubated for 20 min in a cysteine-activated papain solution (200 U, Worthington Biochemicals, Lakewood, NJ) at 37 °C, 5% CO2. The enzymatic reaction was stopped by aspiration of the enzyme and addition of fresh DMEM (see Solutions) with repeated rinsing 2–3 times. Cells were dissociated by trituration using fire-polished, siliconized Pasteur pipettes. The resulting neuron–glia suspension was plated onto

poly-D-lysine-coated glass coverslips and grown in DMEM supplemented with 5% FBS and 2% penicillin/ streptomycin sulfate [15].

2.5. Electrophysiology of OBN primary cultures

Whole-cell recordings from mitral cells (days in vitro, DIV 2–6) were compared between wt (+/+), heterozygous-null (IR+/−), and homozygous-null (IR−/−) mice as described previously for a different line of transgenic mice [16]. Patch pipettes were fabricated from Jencons borosilicate glass (Cat# M15/10, Jencons Limited, Bedfordshire, England) near 1 µm diameter [31] (Narishige, Tokyo Japan). Pipettes were fire-polished, coated near the tip with beeswax to reduce electrode capacitance, and had resistances between 9 and 14 MΩ. Voltage signals were generated and data were acquired using pClamp8.1 software in conjunction with an Axopatch 200B amplifier (Axon instruments, Union City, CA). Cells were held at −80 mV (V_m) and stepped to +40 mV (V_c) for a pulse duration of 400 ms, at a stimulating interval of 30 s to achieve measurements of peak current amplitude, inactivation, and deactivation. To test kinase-induced modulation of Kv1.3 current magnitude, a stable whole-cell recording was established for 4 min before insulin (10 µg/ml) was applied to the bath. Subsequent recordings were collected at 10, 15 and 20 min intervals to achieve a repeated measure statistical design (prior and following insulin application; within cell). Current voltage relationships were assessed by holding the neurons at −90 mV and stepping voltage from −80 to +40 mV in 5 or 10 mV increments for 400 ms using a 40 s interpulse interval to prevent cumulative inactivation [29]. The amplifier output was filtered at 2 kHz, digitized at 2–5 kHz and stored for later analysis.

All electrophysiological data were analyzed using pClamp8.1 software in combination with the analysis packages Origin (Microcal Software, Northampton, MA) and Quattro Pro (Borland International, Scotts Valley, CA). Data traces were subtracted linearly for leakage conductance. The inactivation of the macroscopic current was fit to the sum of two exponentials [$y = y_0 + A_1{}^{(-x/\tau)} + A_2{}^{(-x/\tau)}$] by minimizing the sums of squares, where y_0 was the Y offset, τ_1 and τ_2 were the inactivation time constants and A_1 and A_2 were the amplitudes. The two inactivation time constants or Tau (τ) were combined by multiplying each by its weight (A) and adding the product. The deactivation of the macroscopic current was fit similarly but to a single exponential [$y = y_0 + A_1[(-x/\tau_1)]$]. This type of kinetic analysis is routine for Kv1.3 for both heterologous systems and native expression [12,41].

2.6. Behavioral phenotyping

2.6.1. Acute anosmia experiments—For testing general anosmia, naïve mice were removed from the home cage and placed in a testing cage in which a peanut butter cracker or size-matched marble was hidden from view under the litter. During each trial, the item to be retrieved was randomly selected and hidden in a different location in the cage. The retrieval time was recorded from the time the mouse was released in the center of the cage until the object was found. Experiments were terminated at 10 min and mice were scored that time duration if the object was not retrieved.

2.6.2. Object recognition experiments—Object recognition tests were performed to judge short- (1 h) or longer-term (24 h) memory retention. For the recognition testing, two objects were placed in the chamber and mice were allowed to explore them for a 5 min interval. The amount of time the mouse was oriented to each object within one head length was scored. After either 1 or 24 h, mice were tested for memory retention by replacing two objects in the chamber at the same position, but replacing object 2 with a novel object (object 3) and again scoring orientation for a 5 min interval. The behavioral paradigm was designed based upon that described in Jeon et al. [24]. The percentage of time spent with either two new objects (objects 1 and 2) or one familiar and one novel object (objects 1 and 3) was scored. Percentage

data were transformed by arc-sin transformation and generated means were compared by Student's *t*-test with a 95% confidence level (α≤0.05).

2.6.3. Metabolic chamber experiments—Eight mice of each genotype were monitored for 10 days in shoebox cages ($26 \times 47 \times 13.5$ cm) custom modified for continuous determination of oxygen consumption, locomotor activity, and ingestive behaviors [45]. Briefly, cages were placed inside environmental chambers that provided computer control of ambient temperature (T_a=23 °C) and light cycles. Mixed cage air was sampled for 30 s every 4 min, dried and compressed prior to reaching gas analyzers to determine VO_2. Stiff strain-gauge load beam transducers were attached under two adjacent corners of the cage platform and sampled at 50 Hz to measure changes in the chamber's center of gravity (resolution = 1 mm) allowing localization of the mouse's position in two dimensions. Locomotor activity was defined as unidirectional movement greater than 1 cm and cumulated for dark and light phases. Feeding behavior was monitored by a photobeam sensor across the entrance to the feeder, which was filled with powered chow (Purina 5001; 3.3 kcal/g) and had a 50 ms resolution. Water bottles were positioned in a lick block instrumented to measure contact at the bottle's spout. For each whole-animal physiology property, a 10-day average was computed for each animal, and then the mean value for all animals was analyzed by Student's *t*-test to determine significant difference across the two genotypes with a 95% confidence level (α ≤ 0.05).

3. Results

Gene-targeted deletion of Kv1.3 ion channel results in an increased olfactory ability in terms of both threshold detection and discrimination of odor molecular structure [16]. Because activation of insulin receptor kinase (IR) induces current suppression of Kv1.3 in olfactory bulb neurons [15,17] it was logical to hypothesize that IR heterozygous-null (IR+/−) mice might have an altered olfactory behavior. In a simple test for anosmia, however, age-matched wild-type mice performed the same as those of IR+/− mice (Fig. 1A). The exploratory time to discover a hidden play/non-odor item (marble) was not significantly different between the two genotypes (Student's *t*test, α ≤ 0.05). These data, combined with those demonstrating total exploratory time of objects (Fig. 1B), indicated that the level of motivation to perform a task was not dissimilar between the two genotypes. Likewise, the exploratory time to discover a hidden food/odor item (peanut butter cracker) was not significantly different between the two genotypes (Student's *t*-test, α ≤ 0.05) and was roughly half that needed to retrieve a non-odor item. Therefore, these data indicate that there appeared to be no gross sensory loss.

In order to test more advanced olfactory behaviors it was necessary to test for any memory/ learning deficits in the IR+/− mice to insure equivalent performance. Using a test designed to score short-term and longer-term memory recognition of an object, the IR+/− mice failed to demonstrate recognition of a novel object, whereas the wild-type mice demonstrated significantly different exploration of the novel object, both after 1 h and 24 h (Fig. 1C). Given the fact that the IR+/− did not present any gross anosmia (Fig. 1A) but did have difficulty in memory retention of an object (Fig. 1C), further olfactory behavioral tests were not warranted.

Gene-targeted deletion of Kv1.3 ion channel results in an altered metabolic profile where the mice have a greater locomotor activity, irregular ingestive behaviors, and weigh less [16,47, 48]. The IR+/− mice and age-matched wild-type mice were housed in metabolic chambers for 10 days to measure various daily systems physiology properties including: body weight (g), caloric intake (kcal), fluid intake (g), locomotor activity (m), feeding and drinking events (events/ licks), normalized oxygen consumption (VO_2; ml/min/kg $^{0.75}$), and respiratory quotient (RQ; CO_2/O_2). These properties were calculated separately for the light (0600–1700 h) and the dark (1900–0600 h) cycle with a 2 h down time for cage maintenance and computer

data analysis. As shown in Table 1, none of these physiological parameters were significantly different across the genotypes (Student's t-test, $\alpha \leq 0.05$) with the exception of drinking events.

Olfactory bulbs were harvested as postnatal day 1 (24 h after birth) pups derived from matings between IR (+/−) heterozygous parents and placed into primary cell culture as described in the methodology. There was no qualitative morphological difference in the mitral cell population between the derived genotypes (wild-type, IR+/−, and IR−/−) nor did we find any marked change in longevity of the neurons in culture. When mitral cells were stimulated with a single depolarizing voltage step (V_c = +40 mV) from rest (V_h = −80 mV), the mean peak current amplitude in the heterozygous-null (IR+/−) mice did not significantly vary over days in vitro (DIV), whereas that for the wild-type mice continuously increased over DIV and was significantly greater by DIV 5 (one-way ANOVA, Student– Newman–Keuls (SNK) follow-up test, $\alpha \leq 0.05$; Fig. 2A). Because some biophysical properties of these neurons change with maturation in vitro, particularly that of current density, our data are sorted by DIV for appropriate comparison (Fig. 2B). Previous confocal work in our laboratory has demonstrated that this time window reflects normal increased expression of both the Kv1.3 channel and the IR kinase in wild-type mice [17]. Channel kinetics is known to vary independently of current amplitude, therefore we also compared the rate of Kv1.3 inactivation (τ_{inact}) and deactivation (τ_{deact}) to discern whether there were changes in either of these measured time constants across the two genotypes and across DIV. In both wt mitral cells and those from heterozygous-null (IR+/−) mice, the inactivating portion of the whole-cell current in most records (87%) could be fit by a second order exponential function. The fit τ_{Inact} was not significantly different across genotype for any of the DIV (one-way ANOVA, $\alpha \leq 0.05$; Fig. 2C). Similarly, there was no significant difference across genotype for τ_{deact} with values of 8.1 ± 1.7 ms ($n = 10$) for wt and 6.0 ± 1.4 ms ($n = 6$) for heterozygous-null (IR+/−) (DIV 3–4; Student's $t$test, $\alpha \leq 0.05$). A small fraction of the recorded neurons (8 of 47 cells) could not be properly fit by an exponential decay and had significantly slower activation kinetics with a time to peak current of 300 ms or greater. Since this small fraction of neurons could be found in both wt (+/+) and IR (+/−) mitral cell neuron preparations, and did not significantly vary (in terms of activation kinetics) across genotype regardless of specified holding potential or DIV, they were withheld from any further kinetic analysis. The voltage dependence of Kv1.3 does not appear to be affected by loss of IR kinase gene as demonstrated by overlapping family of current–voltage relations between the genotypes (Fig. 2D). Finally, we tested the effect of insulin in whole-cell recordings obtained from wt (+/+) and IR (+/−) mitral cells to determine if loss of one allele for insulin receptor would alter modulation of Kv1.3 currents. As shown in Fig. 2E, acute insulin stimulation produced a significant decrease in current magnitude in both wt (+/+) and IR (+/−) cells (paired t-test, $\alpha \leq 0.05$). Noteworthy, however, there was no significant difference in inhibitory effect of insulin between the two genotypes (Student's t-test, $\alpha \leq 0.05$).

Because a decrease in peak mitral cell whole-cell current amplitude in response to loss of IR kinase could be attributed to a loss in total Kv1.3 channel protein expression, an alteration by a compensatory current, or alternatively a modulation of Kv channel function, we decided to test for loss of channel protein expression using SDS-PAGE followed by Western blot analysis. Data reported in Fig. 3 demonstrate that there is a 25% reduction in Kv1.3 labeled protein in the OB of IR(+/−) P20 animals in comparison to that of age-matched wt (+/+) animals. Another tyrosine receptor kinase (TrkB) did not demonstrate a change in protein expression between wt (+/+) and IR (+/−) animals (Fig. 3). Because mitral cell neurons from the heterozygous-null animals (IR+/−) show a decrease in current amplitude but not a significant change in kinetics or voltage-dependence, it is conceivable that simply a stepwise loss of channel expression (Fig. 3) rather than a modulation of channel biophysics is responsible for generation of the observed whole-cell current profiles (as seen in Fig. 2A).

4. Discussion

The exploration and development of animal models to study brain function during diabetes mellitus is important to understand the mechanics of the cognitive capacities of these patients. Using an accessible portion of the brain that is rich in both insulin and IR kinase [5,20], we asked whether an imbalance in IR kinase, known to alter the biophysics of the ion channel Kv1.3 [15,17], could perturb electrical signaling and olfactory behaviors driven by this brain region, the olfactory bulb. We know from gene-targeted deletion of the Kv1.3 channel that this channel regulates weight and metabolic balance of the animal as well as restrains olfactory threshold and molecular discrimination of odorants [16,47,48]. Phosphorylation of Kv1.3 by activation of IR kinase could be responsible for driving similar metabolic and olfactory pathways by suppression of channel current rather than genetic channel deletion. Diabetic patients do exhibit loss of olfactory ability [28,43] and poorer performance on memory-based behavioral tasks [21,42]. Lack of Kv1.3 phosphorylation, by reduced IR kinase activation in the brain of these patients, would be consistent with diminished olfactory ability and altered electrical signaling in mitral cells of the olfactory bulb, neurons that normally carry a large proportion of current generated by Kv1.3.

Although homozygous-null IR (−/−) mice could not be raised to adulthood due to development of diabetic ketosis presenting within 24–72 h of life, we expected to observe a degree of olfactory deficit in animals expressing one defective allele of the IR kinase gene (IR+/−). Contrary to our expectation, the IR (+/−) mice did not demonstrate gross olfactory anosmia in comparison to age-matched wt (+/+) animals. Obviously, the heterozygous animals could perform equivalent to their wt counterparts in a task that does not challenge threshold or odor molecular structural discrimination. Tests for anosmia do not detect subtle or refined loss of olfactory ability. Unfortunately, most of the tests designed to explore discreet olfactory acuity (two-choice discrimination paradigms, water-deprivation olfactometers, maze designed discrimination) [8,36,46,49] require learning or memory. Given the evident loss of memory performance in the IR (+/−) for the simple task of novel object recognition, it was not logical to perform such advanced olfactory behavioral phenotyping of the heterozygous-null IR (+/−) that would be negatively biased in performance. Thus the IR (+/−) mice cannot be practically challenged to determine olfactory ability but do demonstrate loss of memory consistent with that known for individuals with diabetes.

Electrophysiological analysis of Kv1.3 current in mitral cells of the olfactory bulb allowed us to characterize the IR (+/−) as well as IR (−/−) genotype if we placed the neurons in primary cell culture prior to severe diabetic ketosis. We could thus determine if there is an inherit change in the electrical excitability of these neurons due to lack of the IR kinase gene that is independent of cellular environment since the neurons would all be placed in a similar in vitro preparation. A stepwise loss of Kv1.3 current magnitude was observed in mitral cell neurons containing one or two alleles of the defective IR kinase gene. In a subset of neurons carrying one allele or none of the defective IR kinase gene, there was no difference in kinase-induced current suppression of the Kv1.3 current, indicating that the heterozygous condition still had some catalytic ability for typical channel modulation. Defective IR kinase activity would predict less basal phosphorylation of the Kv1.3 channel at key Y residues in the cytoplasmic aspect of the channel protein. Thus one might expect that having a defective copy of the IR gene would perhaps alleviate the typical insulin-induced current suppression of Kv1.3, leading to an increase in peak current. However, the seemingly opposite effect of loss of current magnitude with retained kinase-induced suppression led us to probe if altered expression of IR kinase had resulted in altered levels of the channel protein itself. Since, in fact, Kv1.3 channel protein expression in the IR (+/−) mice was reduced by 25% in the olfactory bulb, the lower magnitude of potassium currents in these mice may simply be due to decreased Kv1.3 channel protein. Alternatively, the residual Kv1.3 current could be differentially modulated in

the IR kinase-deficient background or unknown compensatory currents could be contributing to the response profile. Although our data do not allow us to directly discriminate between these alternative hypotheses at this time, in another transgenic line we have characterized, where there is a gene-targeted deletion in Kv1.3, there was not a significant elevation in most other voltage-dependent channels, but rather an increase in several other modulatory kinases in the knockout condition [16]. Interestingly, IR kinase protein expression does not significantly change in Kv1.3-null mice yet the Kv1.3 channel protein is slightly reduced in the IR (+/−) null mice. Furthermore, other Kv1.3 modulating kinases, such as TrkB, are robustly elevated in the Kv1.3-null mice ($6 \times$ increase) but remain unchanged in the IR (+/−) mice (Fig. 3). Again, our data do not allow distinction between these comparisons yet it may be more favorable to surmise that the source of the reduced peak current amplitude in the IR(+/−) and IR (−/−) condition may be more strongly weighted toward Kv1.3 channel expression, than change in tyrosine kinase modulation.

As reported in Accili et al. [1], the lack of IR kinase in these mice does not appear to affect embryonic development even though lack of IR kinase in humans is associated with profound growth retardation [25]. IR (+/−) mice do not demonstrate abnormal glucose tolerance in comparison to wt (+/+) mice yet plasma insulin levels are significantly higher in IR (−/−) than in IR(+/−). Thus there is a metabolic derangement that precipitates death in the IR (−/−) genotype, rather than indicating the role of the IR gene in pre- and post-natal growth. Our metabolic characterization of the IR(+/−) versus wt (+/+) adult mice is consistent with this initial investigation by Accili et al. [1]. Most measurements to assess metabolic energy usage (locomotion, ingestive behaviors, weight, oxygen consumption, and respiratory quotient) were not significantly different between the IR (+/−) and wt (+/+) mice (Table 1). It was our anticipation, based upon known physiology of the diabetic state [35], that the IR (+/−) mice would be heavier, would have a slower metabolism, be less active, and consume more water than their wt (+/+) age-matched counterparts. None of these physiological predictions were borne out by the data; an indication that the IR (+/−) adult mouse may not be a good representative model for human diabetes. The two genotypes did not significantly differ in weight or locomotor activity, the respiratory quotient and normalized oxygen consumption per body weight (VO_2) were equivalent, and the total food consumption and meal events by the animals were not significantly different. The only statistically significant variable between the genotypes was that of pattern of water ingestion. The IR (+/−) mice had a 15% less daily water consumption (although this metric did not reach statistical significance) and had fewer licks (statistically significant), but by deduction, larger swallows (Table 1). Interestingly an identical ingestive behavior was observed in the Kv1.3-null animals, which consumed an equivalent volume of daily water as wt controls, but also took significantly fewer licks [16].

The goal of our experiments was to explore the functional relationship between the modulation of Kv1.3 ion channel protein by IR kinase in an appropriate mouse model with mutation in the insulin signaling pathway. Understanding of the mechanics of cognition during the metabolic disorder diabetes at the level of ion channel biophysics through behavior is a challenging task. It appears that while the IR (−/−) mouse model of diabetes may be useful to tease out metabolic versus growth factor effects of diabetes, reliance on the surviving IR (+/−) adult for behavioral, biochemical, or metabolic analyses does not present a strong enough phenotype for robust determination of the role of insulin signaling for cognition through standard loss of function analysis. Because balance of Kv1.3 function and expression drives metabolism and olfactory discrimination and the activity of Kv1.3 is directly modulated by IR kinase activity, future experiments with other diabetic mouse models [26,32] will be exciting. In lieu of the fact that brain/neuron-specific-targeted deletion of IR kinase is regulated by a promoter that drives weak expression in the olfactory bulb (Khan, personal communication [9]), use of streptozocin-or dietary-induced diabetes may present better models in the understanding of the molecular mechanisms underlying olfactory and cognitive deficits in the diabetic patient.

Acknowledgments

References

1. Accili D, Drago J, Lee EJ, et al. Early neonatal death in mice homozygous for a null allele of the insulin receptor gene. Nat Genet 1996;12:106–109. [PubMed: 8528241]

2. Adamo M, Raizada MK, LeRoith D. Insulin and insulin-like growth factor receptors in the nervous system. Mol Neurobiol 1989;3:71–100. [PubMed: 2553069]

3. Banks WA. The source of cerebral insulin. Eur J Pharmacol 2004;490:5–12. [PubMed: 15094069]

4. Banks WA, Kastin AJ, Pan W. Uptake and degradation of blood-borne insulin by the olfactory bulb. Peptides 1999;20:373–378. [PubMed: 10447096]

5. Baskin DG, Porte D Jr, Guest K, Dorsa DM. Regional concentrations of insulin in the rat brain. Endocrinology 1983;112:898–903. [PubMed: 6337049]

6. Biessels GJ, Kamal Al, Urban IJ, et al. Water maze learning and hippocampal synaptic plasticity in streptozotocin-diabetic rats: effects of insulin treatment. Brain Res 1998;800:125–135. [PubMed: 9685609]

7. Biessels GJ, Kamal A, Ramakers GM, et al. Place learning and hippocampal synaptic plasticity in streptozotocin-induced diabetic rats. Diabetes 1996;45:1259–1266. [PubMed: 8772732]

8. Bodyak N, Slotnick B. Performance of mice in an automated olfactometer: odor detection, discrimination and odor memory. Chem Senses 1999;24:637–645. [PubMed: 10587496]

9. Bruning JC, Gautam D, Burks DJ, et al. Role of brain insulin receptor in control of body weight and reproduction. Science 2000;289:2122–2125. [PubMed: 11000114]

10. Chandy, KG.; Gutman, GA. Voltage-gated potassium channel genes. In: North, RA., editor. Ligand-voltage-gated ion channels. Boca Raton (FL): CRC Press; 1995.

11. Colley BC, Tucker K, Fadool DA. Comparison of modulation of Kv1.3 channel by two receptor tyrosine kinases in olfactory bulb neurons of rodents. Receptors Channels 2004;10:36.

12. Cook KK, Fadool DA. Two adaptor proteins differentially modulate the phosphorylation and biophysics of Kv1.3 ion channel by SRC kinase. J Biol Chem 2002;277:13268–13280. [PubMed: 11812778]

13. Craft S, Watson GS. Insulin and neurodegenerative disease: shared and specific mechanisms. Lancet Neurol 2004;3:169–178. [PubMed: 14980532]

14. Dickson BJ. Wiring the brain with insulin. Science 2003;300:440–441. [PubMed: 12702863]

15. Fadool DA, Levitan IB. Modulation of olfactory bulb neuron potassium current by tyrosine phosphorylation. J Neurosci 1998;18:6126–6137. [PubMed: 9698307]

16. Fadool DA, Tucker K, Fasciani G, et al. Kv1.3 channel gene-targeted deletion produces "super-smeller mice" with altered glomeruli, interacting scaffolding proteins, and biophysics. Neuron 2004;41:389–404. [PubMed: 14766178]

17. Fadool DA, Tucker K, Phillips JJ, Simmen JA. Brain insulin receptor causes activity-dependent current suppression in the olfactory bulb through multiple phosphorylation of Kv1.3. J Neurophysiol 2000;83:2332–2348. [PubMed: 10758137]

18. Folli F, Bonfanti L, Renard E, Kahn CR, Merighi A. Insulin receptor substrate-1 (IRS-1) distribution in the rat central nervous system. J Neurosci 1994;14:6412–6422. [PubMed: 7965046]

19. Gerozissis K. Brain insulin: regulation, mechanisms of action and functions. Cell Mol Neurobiol 2003;23:1–25. [PubMed: 12701881]

20. Gupta G, Azam M, Baquer NZ. Modulation of rat brain insulin receptor kinase activity by diabetes. Neurochem Int 1992;20:487–492. [PubMed: 1339020]

21. Hassing LB, Grant MD, Hofer SM, et al. Type 2 diabetes mellitus contributes to cognitive decline in old age: a longitudinal populationbased study. J Int Neuropsychol 2004;10:599–607.

22. Henneberger C, Grantyn R, Rothe T. Rapid genotyping of newborn gene mutant mice. J Neurosci Methods 2000;100:123–126. [PubMed: 11040374]

23. Jan LY, Jan YN. Cloned potassium channels from eukaryotes and prokaryotes. Annu Rev Neurosci 1997;20:91–123. [PubMed: 9056709]

24. Jeon D, Yang Y-M, Jeong M-J, et al. Enhanced learning and memory in mice lacking Na^+/Ca^{2+} exchanger 2. Neuron 2003;38:965–976. [PubMed: 12818181]

25. Kahn CR. Insulin action, diabetogenes, and the cause of type II diabetes. Diabetes 1996;43:1084.

26. Kitamura T, Kahn CR, Accili D. Insulin receptor knockout mice. Annu Rev Physiol 2003;65:313–332. [PubMed: 12471165]

27. Lannert H, Hoyer S. Intracerebroventricular administration of streptozotocin causes long-term diminutions in learning and memory abilities and in cerebral energy metabolism in adult rats. Behav Neurosci 1998;112:1199–1208. [PubMed: 9829797]

28. Le Flock JP, Le Lievre G, Labroue M, et al. Smell dysfunction and related factors in diabetic patients. Diabetes Care 1993;16:934–937. [PubMed: 8325211]

29. Marom S, Goldstein SAN, Kupper J, Levitan IB. Mechanism and modulation of inactivation of the Kv3 potassium channel. Receptors Channels 1993;1:81–88. [PubMed: 8081714]

30. Matsumoto H, Rhoads DE. Specific binding of insulin to membranes from dendrodendritic synaptosomes of rat olfactory bulb. J Neurochem 1990;54:347–350. [PubMed: 2403434]

31. Mittman SC, Flaming DG, Copenhagen DR, Belgum JH. Bubble pressure measurement of micropipet tip outer diameter. J Neurosci Methods 1987;22:161–166. [PubMed: 3437778]

32. Nandi A, Kitamura Y, Kahn CR, Accili D. Mouse models of insulin resistance. Physiol Rev 2004;84:623–647. [PubMed: 15044684]

33. Papazian DM, Schwarz TL, Tempel BL, Jan YN, Jan LY. Cloning of genomic and complementary DNA from *Shaker*, a putative potassium channel gene from *Drosophila*. Science 1987;237:749–753. [PubMed: 2441470]

34. Park CR, Seeley RJ, Craft S, Woods SC. Intracerebroventricular insulin enhances memory in a passive-avoidance task. Physiol Behav 2000;68:509–514. [PubMed: 10713291]

35. Rhoads, RA.; Tanner, GA. Medical physiology. Vol. 1st ed.. Baltimore: Lippincott: Williams and Wilkins; 1995. p. 706-720.

36. Roman FS, Marchetti E, Bouquerel A, Soumireu-Mourat B. The olfactory tubing maze: a new apparatus for studying learning and memory processes in mice. J Neurosci Methods 2002;117:173–181. [PubMed: 12100983]

37. Sambrook, J.; Fritsch, EF.; Maniatas, T. Molecular cloning: a laboratory manual. New York: Cold Spring Harbor Laboratory; 1989.

38. Song J, Wu L, Chen Z, Kohanski RA, Pick L. Axons guided by insulin receptor in *Drosophila* visual system. Science 2003;300:502–505. [PubMed: 12702880]

39. Sun XJ, Rothenberg P, Kahn CR, et al. Structure of the insulin receptor substrate IRS-1 defines a unique signal transduction protein. Nature (London) 1991;352:73–77. [PubMed: 1648180]

40. Trimmer JS, Rhodes KJ. Localization of voltage-gated ion channels in mammalian brain. Annu Rev Physiol 2004;66:477–519. [PubMed: 14977411]

41. Tucker K, Fadool DA. Neurotrophin modulation of voltage-gated potassium channels in rat through TrkB receptors is time and sensory-experience dependent. J Physiol 2002;542:413–429. [PubMed: 12122142]

42. Watson GS, Craft S. Modulation of memory by insulin and glucose: neuropsychological observations in Alzheimer's disease. Eur J Pharmacol 2004;490:97–113. [PubMed: 15094077]

43. Weinstock RS, Wright HN, Smith DU. Olfactory dysfunction in diabetes mellitus. Physiol Behav 1993;53:17–21. [PubMed: 8434058]

44. Wickelgren I. Cellular neuroscience: tracking insulin to the mind. Science 1998;280:517–519. [PubMed: 9575095]

45. Williams TD, Chambers JB, May OL, et al. Concurrent reductions in blood pressure and metabolic rate during fasting in the unrestrained SHR. Am J Physiol Regul Integr Comp Physiol 2000;278:R255–R262. [PubMed: 10644647]

46. Wilson DA, Stevenson RJ. Olfactory perceptual learning: the critical role of memory in odor discrimination. Neurosci Biobehav Rev 2003;27:307–328. [PubMed: 12946684]

47. Xu J, Koni PA, Wang P, et al. The voltage-gated potassium channel Kv1.3 regulates energy homeostasis and body weight. Hum Mol Genet 2003;12:551–559. [PubMed: 12588802]

48. Xu J, Wang P, Li Y, et al. The voltage-gated potassium channel Kv1.3 regulates peripheral insulin resistance. Proc Natl Acad Sci 2004;101:3112–3117. [PubMed: 14981264]

49. Yee KK, Wysocki CJ. Odorant exposure increases olfactory sensitivity: olfactory epithelium is implicated. Physiol Behav 2001;72:705–711. [PubMed: 11337002]

50. Zhao W, Chen H, Xu H, et al. Brain insulin receptors and spatial memory. Correlated changes in gene expression, tyrosine phosphorylation, and signaling molecules in the hippocampus of water maze trained rats. J Biol Chem 1999;274:34893–34902. [PubMed: 10574963]

51. Zhao WQ, Alkon DL. Role of insulin and insulin receptor in learning and memory. Mol Cell Endocrinol 2001;177:125–134. [PubMed: 11377828]
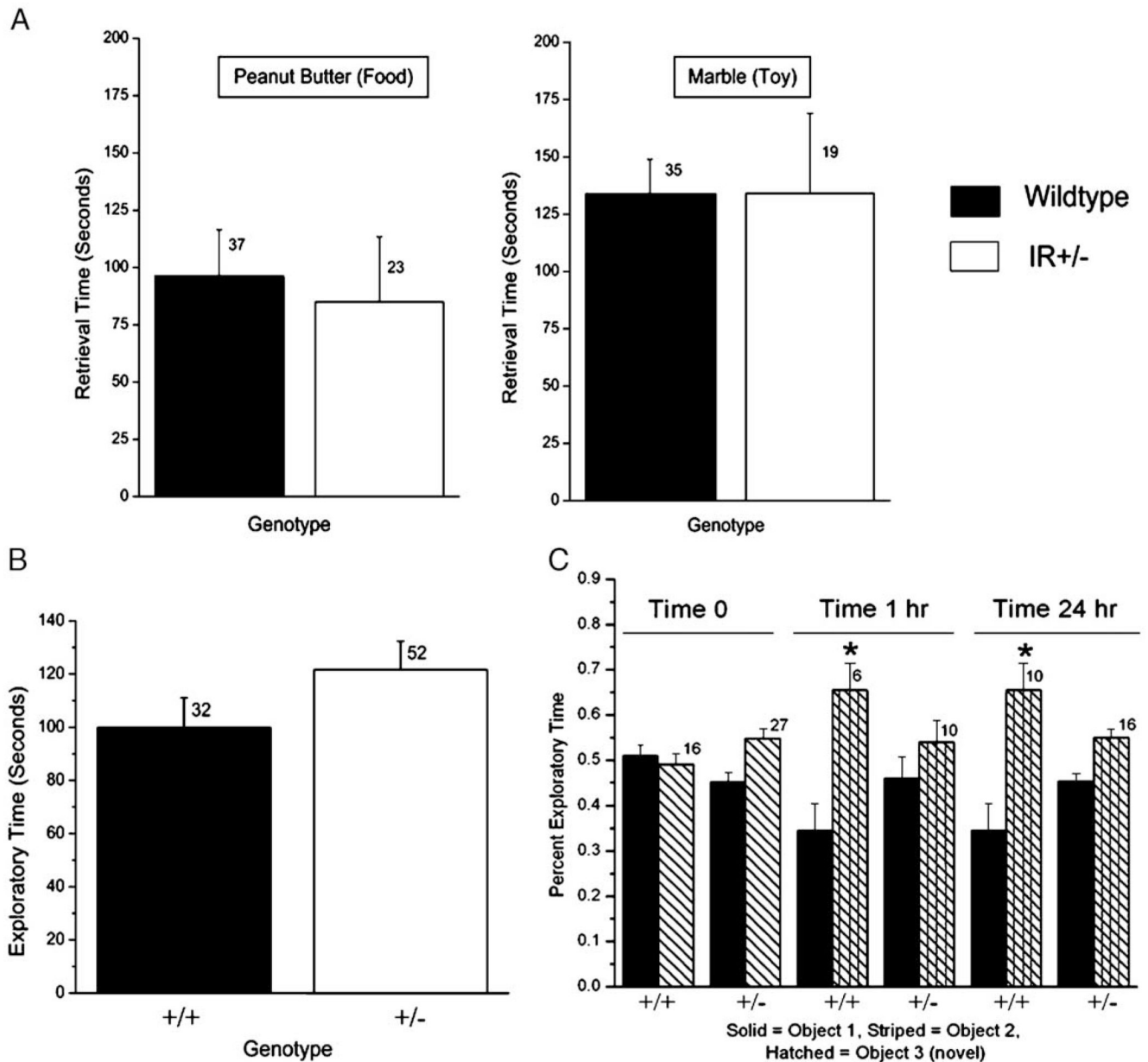
Fig. 1.
Olfactory and memory phenotyping of wild-type and IR kinase (+/−) mice. (A) Histogram plot
of the mean time until retrieval for a hidden play/non-odor item (marble) or a food/odor item
(peanut butter cracker) as a general test for anosmia. Plotted are the mean ± the standard error
of the mean (S.E.M.) for a sample size of mice as noted. Not significantly different, Student's
t-test α ≤ 0.05. (B) Basal motivation for exploration is shown by plotting mean exploratory
time for a novel object for wild-type (+/+) and IR kinase (+/−) mice. Plotted are mean ± S.E.M.
for exploratory times scored during a 5 min interval. Sample sizes (*n*) of naïve mice as indicated;
no significant difference by Student's *t*-test, α ≤ 0.05. (C) Novel object recognition test-results
are plotted for wild-type (+/+) and IR kinase (+/−) mice to determine short- and longer-term
memory. Percent exploratory time of object 1 (solid bar) versus object 2 (striped bar) is
equivalent (0.5) for each genotype upon initial presentation of the objects (Time 0). Percent

exploratory time of two objects following introduction of novel object 3 (hatched bar) to replace object 2 is plotted for a test group of mice tested 1 h (Time 1 h) or 24 h (Time 24 h) after initial object presentation. Plotted are mean ± S.E.M., sample sizes (*n*) as indicated, with statistical significance defined at the 95% confidence level (*), Student's *t*-test with square root transformation for percentile data (arc-sin transformation).
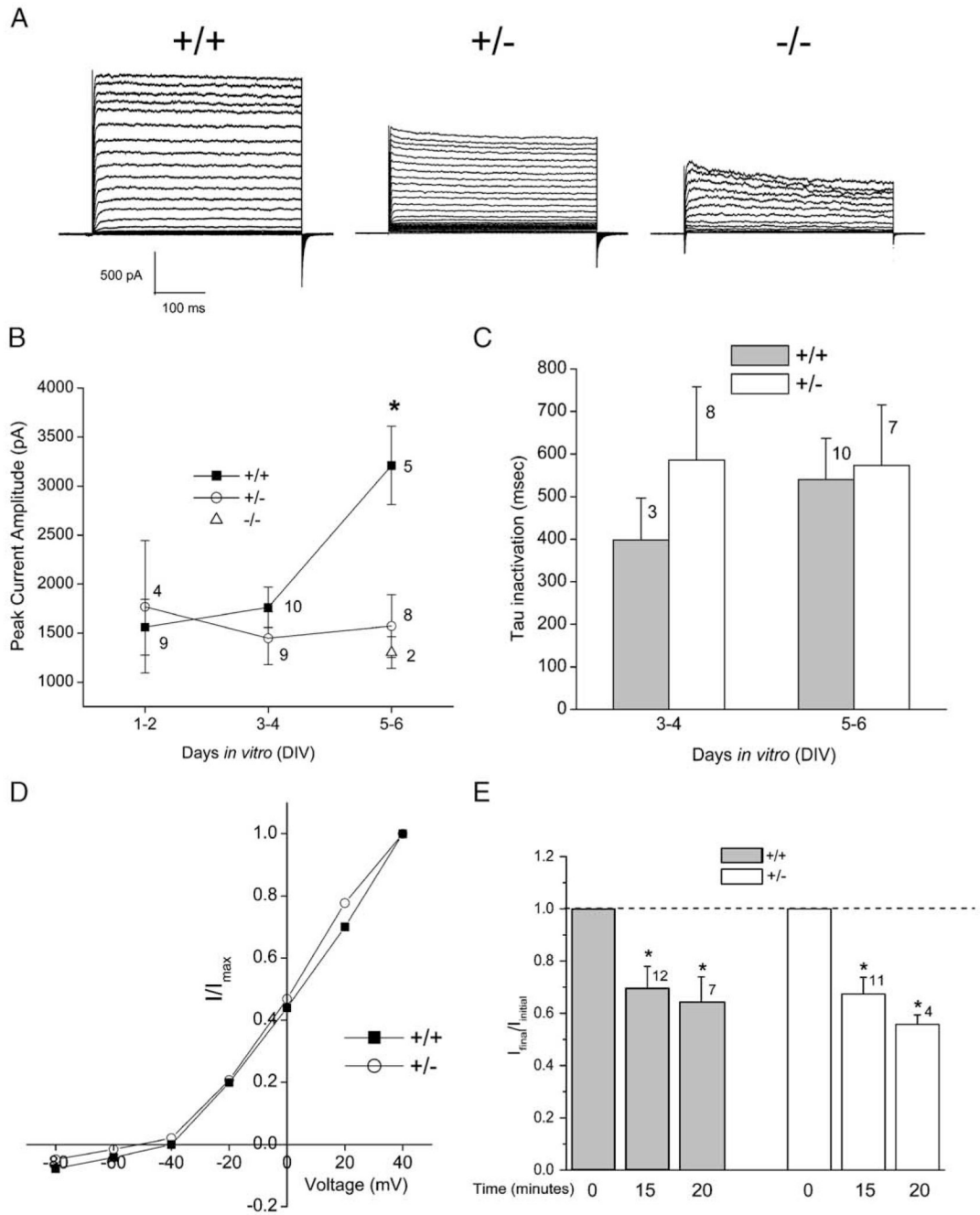
Fig. 2.
Whole-cell voltage– clamp current recordings in mitral cells of the olfactory bulb from wild-type (+/+), IR kinase heterozygous (+/−), and IR kinase-null (−/−) mice. (A) Representative records from a mitral cell voltage-clamped in the whole-cell configuration taken from olfactory bulb neurons (OBNs) cultured from wild-type (+/+) or IR kinase deficient mice (+/−)(−/−). Neurons were held at −90 mV (V_h) and stepped in 5 mV increments (V_c) to a final potential of +5 mV. The duration of pulses was 400 ms with a 40 s interpulse interval to prevent cumulative inactivation of the Kv1.3 channel. Recordings shown are from mitral cells that were 5 days in vitro (DIV5). (B) Peak current magnitude was calculated for a population of mitral cell recordings where neurons were held at −80 mV (V_h) and singly stepped to a depolarizing

potential of +40 mV. Plotted are mean ± S.E.M. with sample size as noted. *Significantly different one-way ANOVA, SNK, $\alpha \leq 0.05$. ■=wild-type, ○=IR (+/−) mice, and Δ=IR (−/−) mice. Statistical analysis did not incorporate IR (−/−)mice due to low sampling size. (C) Histogram graph of the inactivation kinetics (τ) of wild-type (+/+; solid bar) versus IR (+/−) mice (+/−, open bar). Mean ± S.E.M.; no significant difference by one-way ANOVA, $\alpha \leq 0.05$. Voltage stimulation protocol as in panel (B). (D) Normalized current–voltage relation for a representative family of currents evoked by stimulating wild-type and IR kinase deficient neurons. Neurons were held at −80 mV (V_h) and stepped in 20 mV increments (V_c) to a final potential of +40 mV with a 60 s interpulse interval. I =current in pA and I_{max}=maximal current at +40 mV. ■=wild-type, ○=IR (+/−) mice. This current – voltage plot was generated from mitral cells that were DIV 4 – 5 and are representative of 14 such plots. (E) Histogram graph of normalized current (I) elicited by mitral cell neurons of wild-type (+/+; solid bar) versus IR (+/−) mice (+/−; open bar). Voltage paradigm as in (panel B). Whole-cell current recordings were obtained upon breakthrough to the whole-cell configuration ($I_{initial}$), prior to insulin stimulation (Time 0), and after bath application of insulin (10 µg/ml) at the time intervals indicated (Time 15 and Time 20). Dashed line: ratio of $I_{initial}/I_{final}$=1.0 (no change); ratio data are plotted as mean ± S.E.M. *Significantly different by paired t-test, $\alpha \leq 0.05$ for each genotype at independent time points.
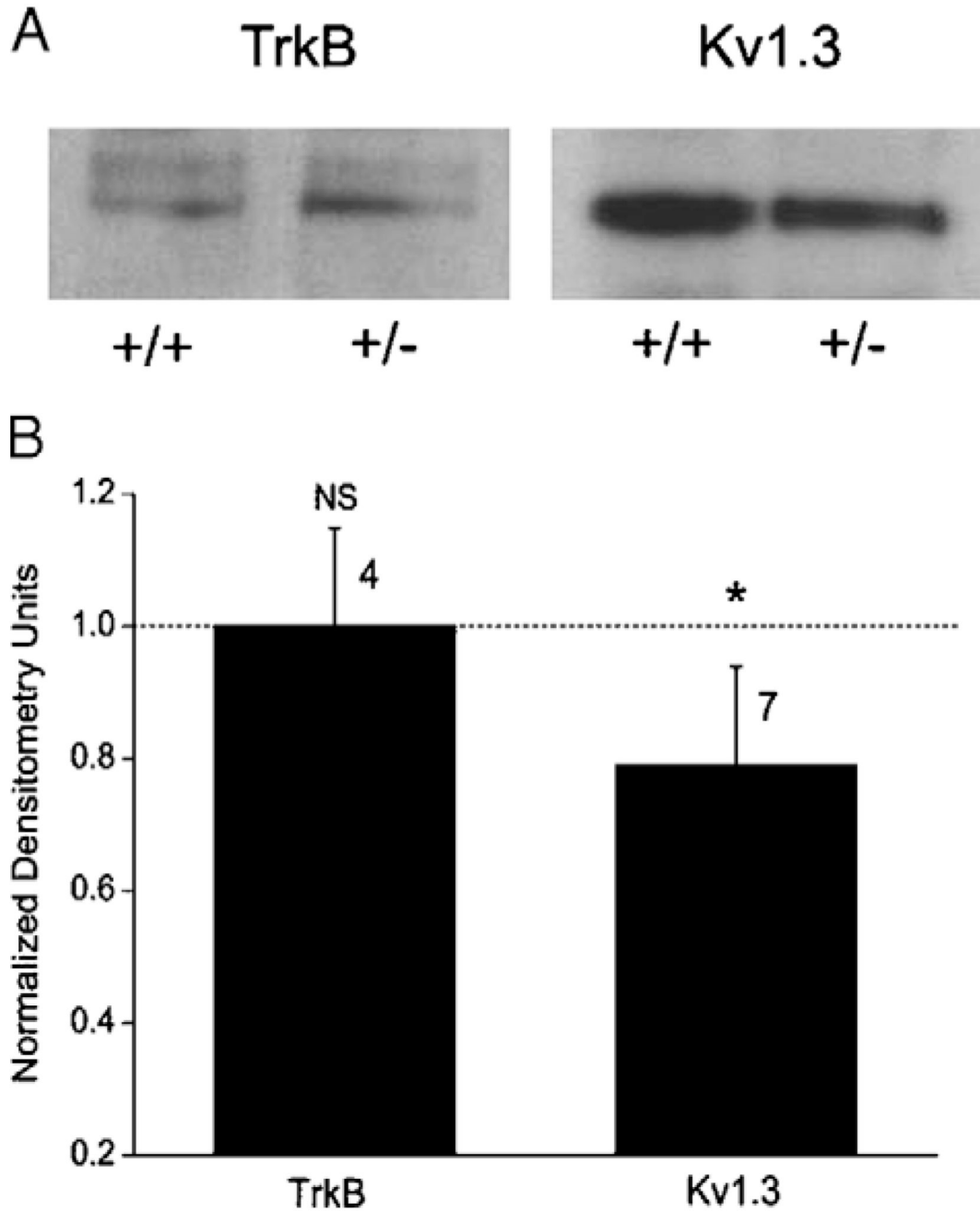
Fig. 3.
Kv1.3 channel protein expression levels in wild-type versus IR kinase (+/−) mice. (A) OB membrane proteins were separated by 10% SDS-PAGE, electro-transferred to nitrocellulose, and blotted with anti-TrkB or anti-Kv1.3 (AU13) to compare expression levels in the wild-type (wt) and IR heterozygous-mice (+/−). (B) Line densitometry was performed within single Western blots to determine pixel density for the neurotrophin receptor (TrkB) and the channel (Kv1.3) protein in the heterozygous and wild-type condition. Immunodensity ratio was calculated as the pixel density of the protein in the mutant mouse over that of the wild-type mouse for proteins exposed on the same piece of nitrocellulose. Mean pixel ratios are plotted mean ± S.E.M.; sample sizes as indicated represent number of isolated pairs of membrane

preparations. Ratio (heterozygous/wild-type) value of 1.0 (dashed line) indicates no difference in expression. *Significantly different by Student's *t*-test with arc-sin transformation for percentage data, $\alpha \leq 0.05$. NS=not significantly different.

Table 1

Comparison of whole-animal physiological properties in wild-type and heterozygous-null IR (+/−) mice as monitored in metabolic chambers for 10 days

Property	Wild-type mice (n =8)	IR (+/−) null mice (n =6)
Body weight (g)	29.6 ± 1.2	29.9 ± 1.4
Caloric intake (kcal)	22.2 ± 4.5	25.9 ± 4.0
Number of food events		
12 h dark	319.2 ± 58	123.2 ± 30
10 h light	253.1 ± 69	162.9 ± 41
Water intake (g)	6.5 ± 0.5	5.5 ± 0.3
Number of licks		
12 h dark	3484.6 ± 316	2201.9 ± 158[*]
10 h light	666.7 ± 106	691.6 ± 198
Normalized VO_2 (ml/min/kg$^{0.75}$)		
12 h dark	30.3 ± 1.2	29.2 ± 0.9
10 h light	24.2 ± 0.7	23.8 ± 0.7
Locomotor activity (m)		
12 h dark	202 ± 30	201 ± 32
10 h light	49 ± 6	59 ± 11

Values are means ± S.E.M. Body weight and caloric and water intakes were measured daily during a 2 h maintenance period just before lights off; all other measures were derived from continuous data collection over ten days accumulated in 30 s intervals and separated into 12 h dark and 10 h light period means.

[*] Significantly different by Student's *t*-test, $\alpha \leq 0.05$.